

# Percolation description of the global topography of Earth and Moon

Abbas Ali Saberi\*

Department of Physics, College of Science, University of Tehran, Post Office Box 14395-547, Tehran, Iran  
 Institut für Theoretische Physik, Universität zu Köln, Zùlpicher Str. 77, 50937 Köln, Germany

(Dated: April 10, 2013)

Remarkable global correlations exist between geometrical features of terrestrial surface on the Earth, current mean sea level and its geological internal processes whose origins have remained an essential goal in the Earth sciences. Theoretical modeling of the ubiquitous self-similar fractal patterns observed on the Earth and their underlying rules is indeed of great importance. Here I present a percolation description of the global topography of the Earth in which the present mean sea level is automatically singled out as a critical level in the model. This finding elucidates the origins of the appearance of scale invariant patterns on the Earth. The criticality is shown to be accompanied by a continental aggregation, unraveling an important correlation between the water and long-range topographic evolutions. To have a comparison point in hand, I apply such analysis onto the lunar topography which reveals various characteristic features of the Moon.

PACS numbers: 91.10.Jf, 64.60.ah, 96.20.-n

Discovering the connection between geometrical features of terrestrial surface on the Earth and its geological internal processes has long been a basic challenge area in the Earth sciences [1, 2], and attracted the attention of physicists and mathematicians as well [3]. Various theoretical models have emerged to identify the underlying constructive rules responsible for the appearance of self-similarity, scale and conformal invariance in the fractal geometry of the local geomorphic patterns [4–9]. In comparison with different models proposed to describe the statistical properties of regional features [10–12], the global topography has received less attention and thus remained controversial. Here I show that the global surface topography can be well described by percolation theory, the simplest and fundamental model in statistical mechanics that exhibits phase transitions. A dynamic *geoid*-like level is defined as an equipotential spherical surface as a counterpart of the percolation parameter. The analysis shows a geometrical phase transition in which the critical level surface directly corresponds to the present mean sea level on the Earth, automatically singling this level out. This may shed new light on the tectonic plate motion and help unravel the dynamic story of the Earth's interior. As a comparison, I also present its application to the lunar topography.

Scale invariance is a remarkable feature of the Earth surface topography. Observations [13–16] indicate that, over a wide range of scales, the power spectrum  $S$  of linear transects of the Earth's topography follows the scaling relation  $S \propto k^{-2}$  with the wave number  $k$ . Such a power law spectrum in the topography leads to the corresponding iso-height lines (such as coastlines) being fractal sets characterized by a dominant fractal dimension of  $4/3$  [3, 4, 17]. Many other ubiquitous scaling relations observed in the various terrestrial features e.g., in the radiation fields of volcanoes [18, 19], surface magnetic susceptibility [20], geomagnetism [21] and surface hydrology such as in the river basin geomorphology [22] are all rele-

vant to the wide range scale invariance of the topography. Nevertheless, further surveys based on fractional Brownian motion (fBm) model [14] of topography/bathymetry [36] revealed a more complex multifractal structure of the Earth's morphology giving rise to distinct scaling prop-

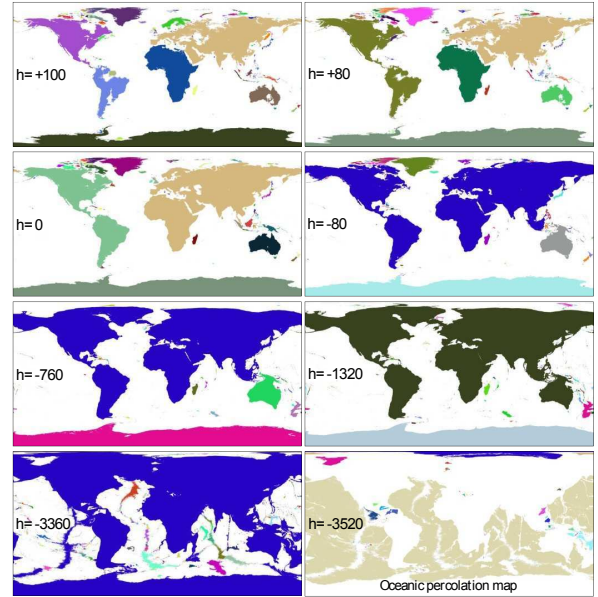


FIG. 1: (Color online) Schematic illustration of the continental aggregation by decreasing the sea level from top to bottom. The first four snapshots are selected around the remarkable percolation transition at the present mean sea level around which the major parts of the landmass join together. This is followed by three other levels indicating the junction of the Greenland, Australia and Antarctica to the giant landmass. The lowest right figure shows the longitudinal percolation of the oceanic clusters (see the supplementary material for enlarged figures and also the ones at additional sea levels).

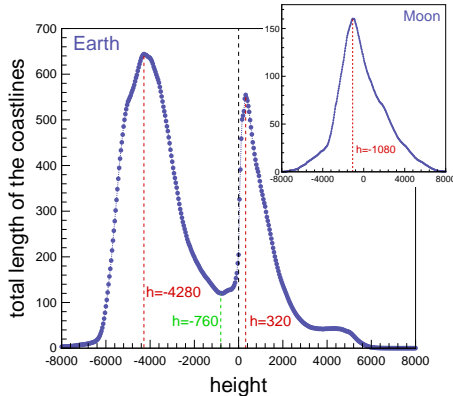


FIG. 2: (Color online) The total length of the coastlines as a function of the sea level (or height) for the Earth (main panel) and the Moon (inset).

erties of oceans, continents and continental margins [7]. Such a difference is also evident in the well-known bimodal distribution of the Earth's topography [23] that reflects the topographic dichotomy of continents and ocean basins, a consequence of plate tectonic processes.

Plate tectonic theory provides a framework that explains most of the major surface topographic features of the Earth. It also accounts for the connection between the processes that facilitate heat loss and the forces that drive plate motion. The distribution of the plate areas covering the Earth has been shown to be a power law with exponent  $\sim 0.25$  for all plates [24, 25]. A remarkable relationship that provides one of the cornerstones of plate tectonics is that, to a very good approximation, the depth of the ocean floor beneath the ridge crest increases with square root of the age of the ocean floor, at least for ocean lithosphere younger than about 80 Myr ago [26]. It plays an important role in topographical changes and fundamentally affects long-term variations in global sea level that would assume a surface equal to the geoid. Here I present the results of a statistical analysis based on percolation theory that provides new insight into the better understanding of various interrelationships between the above mentioned issues and their origins.

I use the topographic data available for the global relief model of the Earth's surface that integrates land topography and ocean bathymetry [27] (the data information is presented in <http://www.ngdc.noaa.gov/mgg/global/global.html>). Current mean sea level is assumed as a vertical datum of the height relief which means that the data considers the imperfect ellipsoidal shape of the Earth. The height relief  $h(r, \theta, \phi)$  is therefore assumed on a sphere of unit radius  $r = 1$ , that also coincides with the present mean sea level (as zero height level) on the Earth. All

corresponding lengths here are expressed in units of the Earth's average radius.

Now imagine flooding this global landscape in a way that the continental land masses were criss-crossed by a series of narrow channels so that the resulting sea level all over the Earth would coincide with a spherical surface—the geoid. All parts above the water level are then colored differently as disjoint islands, and the rest is left white (Fig. 1). If the water level is high, there will be small disconnected islands, and if it is low, there will be disconnected lakes. However, there may be a critical value of the sea level  $h = h_c$  at which a percolation transition takes place [28, 29].

The percolation problem [29, 31] is an example of the simplest pure geometrical phase transitions with nontrivial critical behavior, and it is closely related to the surface topography [32, 33]. At the critical point in two dimensions, the percolation clusters are some fractal objects whose outer perimeter is described by a fractal dimension of  $4/3$ . By considering the dynamic sea level (height) as a percolation parameter, I examine a possible description of Earth's topography by means of the percolation theory.

The first quantity of interest is the total length of the coastlines at varying altitude (or sea level) which is shown in Fig. 2. In all figures, the error bars are of the same order as the symbol size [37]. Having looked at Fig. 2, this quantity closely resembles the height distribution function of the Earth and the Moon [30]. The one for the Earth is characterized by the presence of two lev-

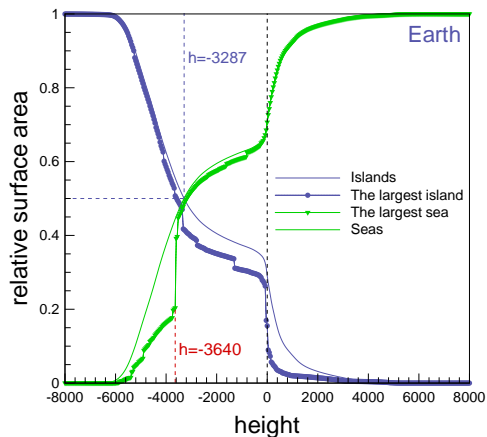


FIG. 3: (Color online) Relative surface area of the largest island (circles) and the largest sea (triangles) followed by the total surface area of the islands and the oceans (solid lines) to the total area  $4\pi$  of the Earth, as a function of the sea level. One critical level is distinguished by each order parameter. The oceanic critical level is close to the level  $h = -3287$  m at which the total island and oceanic surface areas are equal.

els centered around the elevations 320 m and  $-4280$  m in the continental platforms and oceanic floors, respectively. The ratio of the total length of the coastlines at 320 m to the zero height level is  $\sim 2.71$ . Unlike Earth, the Moon's curve features only a single peak at around  $-1080$  m.

The usual order parameter is defined as the probability of any site to be part of the largest island. As shown in Fig. 3, the order parameter for islands has a sharp drop-off around the zero height level i.e., right at the present mean sea level. According to the further evidence given in the following, it is an indicative of a geometrical phase transition at this level. The same analysis for the oceanic clusters (where disjoint oceans at each level are differently colored, leaving islands white) gives rise to a discontinuous jump in the oceanic order parameter at around  $-3640$  m (Fig. 3).

Figure 4 illustrates two other percolation observables measured for the Earth, the mean island size (analogous to the susceptibility of the system), and the correlation length. The mean island size  $\chi$  is defined as  $\chi = \sum'_s s^2 n_s(h) / \sum'_s s n_s(h)$ , where  $n_s(h)$  denotes the average number of islands of size  $s$  at level  $h$ , and the prime on the sums indicates the exclusion of the largest island in each measurement. The correlation length  $\xi$  is also defined as average distance of sites belonging to the same island,  $\xi^2 = \sum'_s 2R_s^2 s^2 n_s(h) / \sum'_s s^2 n_s(h)$ , where  $R_s$  is the radius of gyration of a given  $s$ -cluster. As shown in Fig. 4, both quantities  $\chi$  and  $\xi$  become divergent at the present mean sea level. The divergence of the correlation length is a signature of a continuous phase transition at this level, implying that the critical fluctuations dominate at each length scale and that the system becomes scale invariant. These results provide a strong correlation between the water and long-range topographic evolutions on the Earth. Nevertheless, one may imagine a model in which water itself—through erosion, evaporation, precipitation and sedimentation, etc.—may have an active role in shaping topography i.e., the activity of water itself with resulting plains of little height, shapes the landscape to appear critical around the zero height.

The measurement of  $\chi$  and  $\xi$  for the oceanic clusters shows a dominant divergence that signals the oceanic critical level already observed in Fig. 3. The mean ocean size reaches its absolute maximum at this critical level and the correlation length remains approximately constant at its maximum for level interval  $-4280 \lesssim h \lesssim -3760$  (see the supplementary material).

Figure 1 gave an illustration of the percolation transition at the present mean sea level. As can be seen from the figure, all major continental junctions occur at the level interval  $-80 \lesssim h \lesssim +80$ . At a sea level around  $-760$  m, Greenland joins the Afro-Eurasia supercontinent to the Americas and at the same level the total length of the coastlines reaches its minimum (Fig. 2). Australia and Antarctica continents join to the landmass

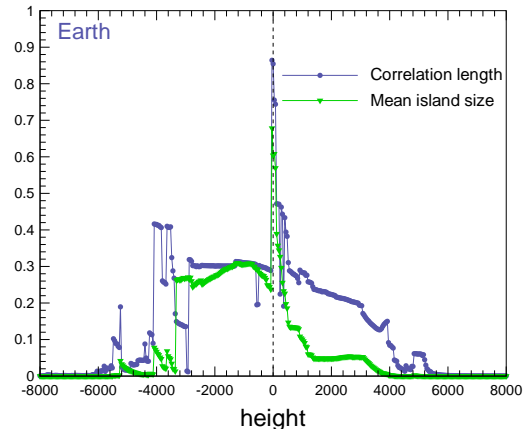


FIG. 4: (Color online) Correlation length and mean island (land) size vs the sea level, with a remarkable characterization of a geometrical phase transition at the present mean sea level (zero height level). The scale factors by which all the numbers labeling the vertical axis should be multiplied to get the correct graph units are the radius and the square of the radius of the Earth for  $\xi$  and  $\chi$ , respectively.

at  $-1320$  m and  $-3360$  m, respectively (Fig. 1).

In order to have a reference point for comparison, as an example of the most heavily studied waterless body with a completely different surface properties and interior mechanism, let me analyze the lunar topography. I used the topogrd2 data set (accessible from <http://pds-geosciences.wustl.edu/missions/clementine/gravtopo.html>), which is measured relative to a spheroid of radius 1738 km at the equator—the zero height level. I rescale the Moon's average radius to 1.

The percolation observables discussed above for the islands are measured as a function of a hypothetical sea level (Fig. 5). The order parameter shows two rather small jumps at altitude levels around  $-960$  m and  $1360$  m. The correlation length and the mean island size have also two dominant peaks at these levels (see the inset of Fig. 5).

The Moon's height distribution function features a single global peak at level  $\sim -950$  m which is quite close to the one of the critical levels located at  $\sim -960$  m. In addition, if we measure the correlation length and the mean cluster size for the oceanic clusters, they show only one critical level very close to the one located at  $\sim -960$  m. These may imply that this critical level is more important for the description of the global topography of the Moon. This is also quite close to the level  $h = -1049$  m at which the total island and oceanic surface areas are equal, meaning that the island and oceanic percolation thresholds coincide.

The illustrative figure 6 shows the connectivity of the islands on both sides of the critical level. At a height level  $h = -950$  m, a little above the critical level, there exists a number of disjoint islands. At slightly below the critical level at  $h = -1050$  m, the islands merge together to form a giant percolating island which spans the Moon in the longitudinal direction.

Nevertheless, the other critical level at  $h = 1360$  m, unravels a characteristic feature of the lunar farside. As it is known, one of the most striking geological features of the Moon is the elevation dichotomy [34] between the hemispheres: the nearside is low and flat, dominated by volcanic maria, whereas the farside is mountainous and deeply cratered. The illustrations in Fig. 6 for elevation levels at  $h = 1360$  and  $1340$  m, at both sides of the critical level, indicate the aggregation of two main mountainous islands that are separated by a very narrow passageway. This may be a benchmark of a rather non-random origin of the formation of the lunar farside highlands [35].

To summarize, the percolation description of the global Earth's topography uncovers the important role that is played by the water on the Earth. The critical threshold of the model coincides with the current mean sea level on the Earth. This criticality is along with a sign of the continental aggregation at this level which seems to be more dominated by the *endogenic* processes (like volcanic activity, Earthquakes and tectonic processes) originat-

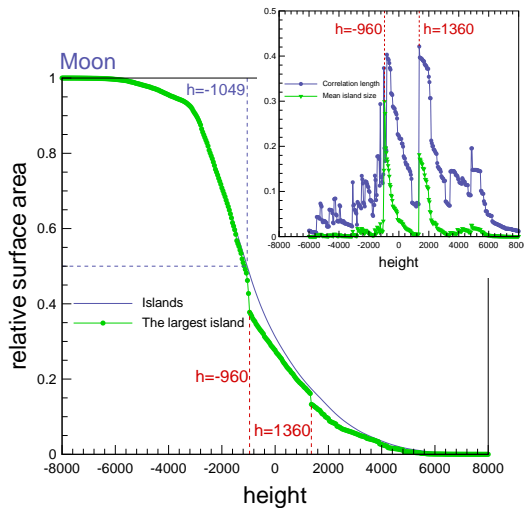


FIG. 5: (Color online) Relative surface area of the largest island followed by the total surface area of the islands to the total area  $4\pi$  of the Moon, as a function of the hypothetical sea level. At level  $\sim -1049$  m, the total island and oceanic surface areas on the Moon are equal. The two jumps in the order parameter at levels around  $-960$  m and  $1360$  m are also decoded in the divergent behavior of the correlation length and the mean island size (the inset). Such two jumps are unusual for percolation.

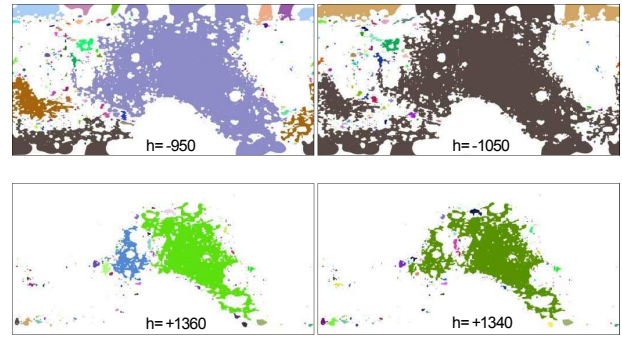


FIG. 6: (Color online) Upper: disjoint islands with heights higher than the hypothetical sea level on the Moon for two different levels  $h = -950$  m and  $-1050$  m, slightly above and below the critical level, respectively. Appearance of the spanning island (right figure) is an indicative of a percolation transition. Lower: aggregation of the two main mountainous islands at the lunar farside around the second critical level at  $\sim 1360$  m.

ing within the Earth that are mainly responsible for the very long-wavelength topography of the Earth's surface, rather than by the *exogenic* processes like erosion, weathering and precipitation. The criticality of the current sea level also justifies the appearance of the scale (and conformal) invariant features on the Earth with an intriguing coincidence of the dominant  $4/3$  fractal dimension in the critical model and observation. The main critical level for the Moon has the same amount of land and oceans at the threshold, indicating a purely geometrical phase transition.

I would like to thank J. Cardy, M. Kardar, J. Krug, T. Quella and M. Sahimi for their many useful comments, and especially thank D. Stauffer for his many helpful comments and suggestions. The author also thanks H. Dashti-Naserabadi for his kind help with programming and M.J. Fallahi for the Earth's data source. Financial support from the Deutsche Forschungsgemeinschaft via SFB/TR 12 and supports from Alexander von Humboldt Foundation, are gratefully acknowledged. I also acknowledge partial financial supports by the research council of the University of Tehran.

\* Electronic address: [ab.saberi@ut.ac.ir](mailto:ab.saberi@ut.ac.ir)

- [1] C. Lyell, *The Principles of Geology; or, the Modern Changes of the Earth and its Inhabitants Considered as Illustrative of Geology*, vol. **3**, Murray, London (1830).
- [2] A. Cazenave, A. Souriau and K. Dominh, *Nature* **340**, 54-57 (1989).
- [3] J. Perrin, *Les atomes*, NRF-Gallimard, Paris (1913).
- [4] B. B. Mandelbrot, *Science* **156**, 636-638 (1967).
- [5] B. B. Mandelbrot, *The Fractal Geometry of Nature*, W. H. Freeman, New York (1983).



- [6] J.-S. Gagnon, S. Lovejoy and D. Schertzer, *Europhys. Lett.* **62**, 801-807 (2003).
- [7] J.-S. Gagnon, S. Lovejoy and D. Schertzer, *Nonlinear Processes Geophys.* **13**, 541-570 (2006).
- [8] A. Baldassarri, M. Montuori, O. Prieto-Ballesteros and S. C. Manrubia, *J. Geophys. Res.* **113**, E09002 (2008).
- [9] G. Boffetta, A. Celani, D. Dezzani and A. Seminara, *Geophys. Res. Lett.* **35**, L03615 (2008).
- [10] C. P. Stark, *Nature* **352**, 423-425 (1991).
- [11] A. Maritan, F. Colaiori, A. Flammini, M. Cieplak and J. R. Banavar, *Science* **272**, 984-986 (1996).
- [12] B. Sapoval, A. Baldassarri and A. Gabrielli, *Phys. Rev. Lett.* **93**, 098501 (2004).
- [13] F. A. Vening Meinesz, *Proc. Koninkl. Ned. Akad. Wetensch. ser. B* **55**, 212-228 (1951).
- [14] B. Mandelbrot, *Proc. Nat. Acad. Sci. U.S.A.* **72**, 3825-3828 (1975).
- [15] R. S. Sayles and T. R. Thomas, *Nature* **271**, 431-434 (1978).
- [16] J. D. Pelletier, *J. Geophys. Res.* **104**, 7359-7375 (1999).
- [17] H. Steinhaus, *Colloquium Mathematicum*, III, 1-13 (1954).
- [18] D. C. Harvey, H. Gaonach, S. Lovejoy, J. Stix and D. Schertzer, *Fractals* **10**, 265-274 (2002).
- [19] H. Gaonach, S. Lovejoy and D. Schertzer, *Int. J. Rem. Sens.* **24**(11), 2323-2344 (2003).
- [20] M. Pilkington and J. Todoeschuck, *Geophys. Res. Lett.* **22**, 779-782 (1995).
- [21] S. Pecknold, S. Lovejoy and D. Schertzer, *Geophys. J. Inter.* **145**, 127-144 (2001).
- [22] I. Rodriguez-Iturbe and A. Rinaldo, *Fractal River Basins: Chance and Self-Organization*, Cambridge University Press, Cambridge (1997).
- [23] A. Wegener, *The origin of continents and oceans*. In: J. Biram (Ed.), *Trans. from the 1929 4th German edn.* New York, Dover, 246pp (1966).
- [24] P. Bird, *Geochemistry Geophysics Geosystems* **4**(3), 1027 (2003).
- [25] D. Sornette and V. F. Pisarenko, *Geophys. Res. Lett.* **30**, 1105 (2003).
- [26] D. L. Turcotte and G. Schubert, *Geodynamics, Application of Continuum Physics to Geological Problems*, John Wiley, New York (1982).
- [27] C. Amante and B. W. Eakins, *ETOPO1 1 Arc-Minute Global Relief Model: Procedures, Data Sources and Analysis*. NOAA Technical Memorandum NESDIS NGDC-24, 19 pp (March 2009).
- [28] J. Cardy, *Nature physics* **2**, 67-68 (2006).
- [29] M. Sahimi, *Applications of Percolation Theory*, Taylor & Francis, London (1994).
- [30] P. R. Stoddard and D. M. Jurdy, *Icarus* **217**, 524-533 (2012).
- [31] D. Stauffer and A. Aharony, *Introduction to Percolation Theory*, 2nd ed. Taylor & Francis, London (1994).
- [32] A. A. Saberi, M. A. Rajabpour and S. Rouhani, *Phys. Rev. Lett.* **100**, 044504 (2008).
- [33] A. A. Saberi, *Appl. Phys. Lett.* **97**, 154102 (2010).
- [34] M. T. Zuber, D. E. Smith, F. G. Lemoine and G. A. Neumann, *Science* **266**, 1839-1843 (1994).
- [35] M. Jutzi and E. Asphaug, *Nature* **476**, 6972 (2011).
- [36] bathymetry is the underwater equivalent to topography.
- [37] The ETOPO1 global relief model has an accuracy of about 10 meters at best, likely less accurate in the deep ocean. Part of the reason for the large error bars are that each cell's elevation value represents the average elevation over the entire roughly  $2 \times 2 \text{ km}^2$  footprint of the cell [27]. All mentioned height levels here would indeed bear such uncertainties.